JOURNAL OF MATERIALS SCIENCE 15 (1980) 2985–2990

Steady-state creep behaviour of Ti_3Al-base intermetallics

M. G. MENDIRATTA
Systems Research Laboratories Inc., 2800 Indian Ripple Road, Dayton, Ohio 45440, USA

H. A. LIPSITT
Air Force Wright Aeronautical Laboratories Materials Laboratory, Wright–Patterson Air Force Base, Ohio 45433, USA

The steady-state creep behaviour of Ti_3Al and Ti_3Al + 10 wt% Nb was studied in the temperature range 550 to 825° C and in the stress range 69 to 312 MN m^{-2}. The temperature and stress dependences of the steady-state creep rates were determined for both intermetallics, and the activation energy and stress-exponent were measured. At temperatures above 700° C, the stress dependence of the steady-state creep rate indicated two distinct creep regimes: at stresses above 138 MN m^{-2}, the creep was controlled most probably by dislocation climb; at stresses below 138 MN m^{-2}, a transition regime with a lower stress-exponent value was obtained.

1. Introduction

Considerable research efforts are presently being directed toward development of α_2-phase titanium aluminides as structural materials for aircraft turbine engines. The α_2-phase is based upon the composition Ti_3Al and has an ordered DO_{19}-type lattice structure. Recent work [1] has shown that the Ti_3Al-base alloys, although brittle at low temperatures, retain reasonable strength levels up to 800° C. At about 550° C the alloys begin to exhibit measurable ductility which increases gradually with increasing temperature. The tensile deformation modes in Ti_3Al have been studied by Williams and Blackburn at room temperature [2] and by Sastry and Lipsitt at 700° C [3]. The main findings of these investigations are that slip in Ti_3Al is highly planar and is comprised mostly of $\frac{a}{6}\langle 11\bar{2}0\rangle$-type ("$a$") dislocations. A few $\frac{a}{6}\langle 11\bar{2}6\rangle$-type ("$c + a$") dislocations have also been observed [2]. The ordered lattice structure and restriction of slip systems observed in Ti_3Al appear to be responsible for both the high-temperature strength and the low-temperature brittleness. Ordering-transformations [3] and strain-amplitude controlled cyclic deformation [4] studies have also been carried out recently on Ti_3Al-base intermetallics.

The present investigation is directed toward an understanding of the steady-state creep behaviour in Ti_3Al-base materials in the stress and temperature ranges which correspond to practical applications. This goal was pursued by establishing the stress and temperature dependences of the steady-state creep rates.

2. Experimental procedure

Two intermetallics were used in this investigation: the near-stoichiometric Ti_3Al (of nominal composition Ti–16 wt% Al) and Ti_3Al + 10 wt% Nb (of nominal composition Ti–16 wt% Al–10 wt% Nb). Nb is added in the Ti_3Al-base alloy primarily to improve the oxidation resistance; significant improvement has been shown to occur [5] with the addition of 5 to 10 wt% Nb. The alloys used in this study were cast as rod ingots and converted by Nuclear Metals Inc., to a powder form of −35 mesh using a rotating electrode process. The powders were packed in Ti–6Al–4V cans, evacuated, sealed, and hot-extruded at 1200° C with an extrusion ratio of 26:1. The details of the extrusion process, the method of specimen machining, and the geometry of the specimen are described in a recent paper [6]. The machined specimens were given an annealing treatment of

0022–2461/80/122985–06$02.60/0

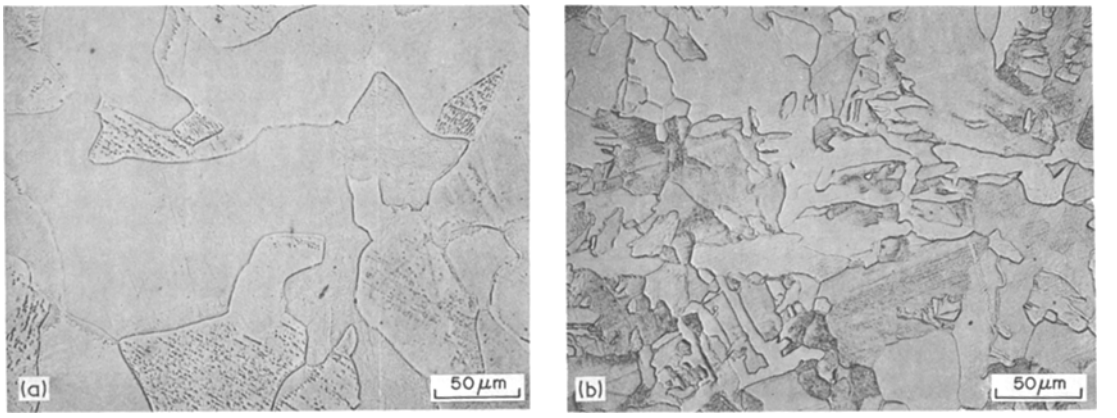

Figure 1 (a) Microstructure of extruded and heat-treated Ti–16 wt% Al. Extrusion is followed by heat treatment at 1000° C for 4 h and then furnace cooled. (b) Light micrograph showing microstructure of extruded and heat-treated Ti_3Al + 10 wt% Nb. Extrusion is followed by heat treatment at 1000° C for 4 h and then air cooled.

1000° C for 4 h in vacuum, in order to stabilize the microstructure, and were then furnace cooled.

A lever-type constant-load creep machine was utilized for the creep experiments. The tests were performed in air at stresses ranging from 69 to 312 MN m^{-2} and at temperatures ranging from 550 to 825° C. During the creep tests the temperature was controlled to within ± 2° C. Most of the tests were carried out at constant (nominal) stresses; however, in some tests, stress levels were increased on the same specimen after the onset of steady-state creep. In all experiments the steady-state creep regimes were observed to be well established below 2% total strain. Thus, the correction necessary to convert the nominal stress to true stress was very small and, therefore, neglected. In the creep experiments the specimen elongation was continuously recorded by means of a linear variable differential transformer (LVDT) and a mechanical extensometer clamped onto the flanges of the specimens. After the creep had proceeded well into the steady-state regimes, creep tests were discontinued and specimens cooled under load to minimize recovery of the deformation structures.

3. Results and discussion

3.1. Microstructures of the heat-treated intermetallics

The microstructures of the extruded and subsequently heat-treated Ti_3Al and Ti_3Al + 10 wt% Nb are shown in the light micrographs of Fig. 1a and b, respectively. For Ti_3Al the heat treatment produced a nearly equiaxed grain structure (with average grain size approximately 100 μm) with some jagged grain boundaries. For Ti_3Al + 10 wt% Nb the microstructure consisted of highly irregular (non-equiaxed) grains having very jagged boundaries. Also in Ti_3Al + 10 wt% Nb the average grain size was smaller (about 60 μm) than that in Ti_3Al. It appears that Nb additions in Ti_3Al retard the diffusive processes required for recrystallization and grain growth. Polished specimens of both intermetallics were scanned using the electron microprobe over distances up to 1 mm; the characteristic X-ray intensities corresponding to Ti, Al, and Nb did not exhibit compositional heterogeneities. TEM bright-field and selected-area diffraction examination of thin foils revealed the presence of only the ordered α_2-phase in both the Ti_3Al and Ti_3Al + 10 wt% Nb. In Ti_3Al the grains contained a very low density of dislocations and were uniformly recovered. In Ti_3Al + 10 wt% Nb, however, while some of the grains were observed to be nearly fully recovered, most of them consisted of aligned, rather thin, long sub-grains. Most of the sub-boundaries were simple tilt boundaries containing *a*-type dislocations; however, some consisted of *a*-type dislocation networks. The long sub-grain morphology is thought to be the result of partial annealing of the martensitic substructure that formed during cooling in Ti_3Al + 10 wt% Nb after the extrusion process [3]. The martensitic transformation is related to the stabilization of a high-temperature b c c β-phase due to the addition of Nb in Ti_3Al; in Ti_3Al without Nb the furnace cooling is not sufficiently fast to produce a martensitic transformation [3].

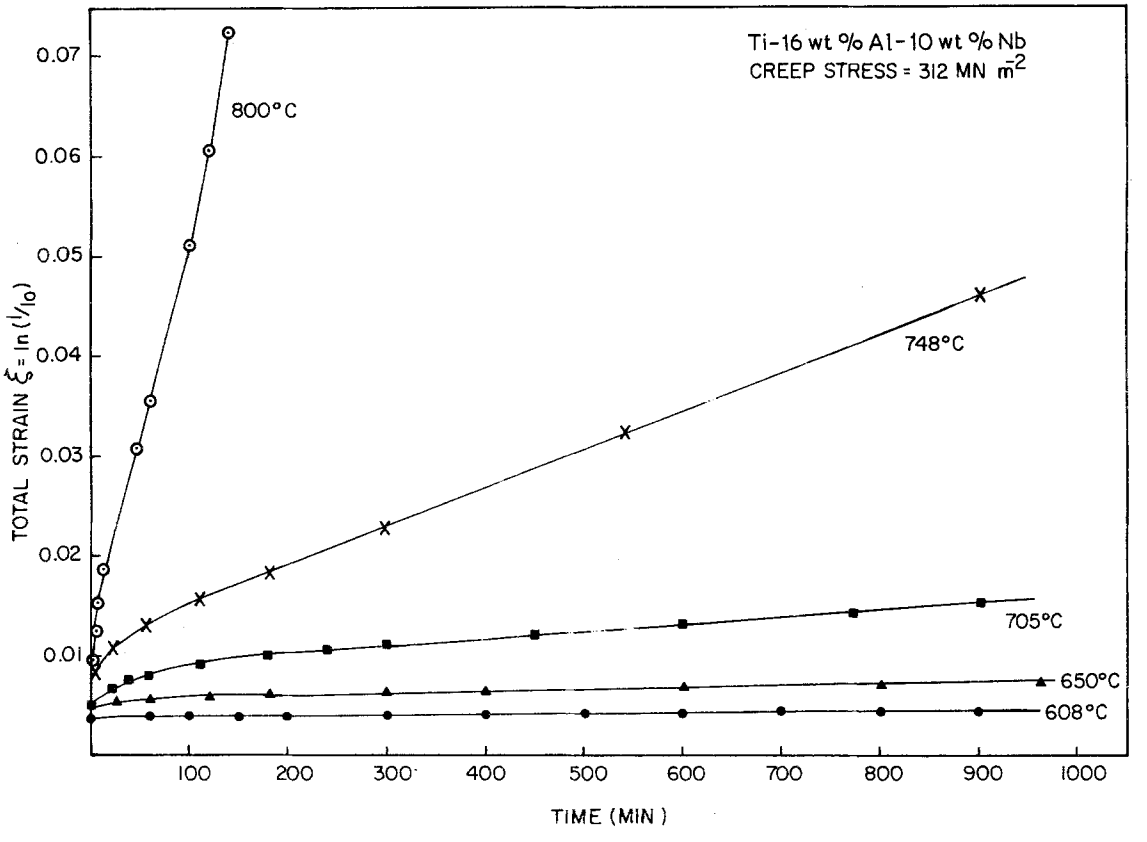

Figure 2 Creep curves for Ti_3Al + 10 wt% Nb.

3.2. Creep curves

Fig. 2 is an example of the type of creep exhibited by the intermetallics. At all stresses and temperatures utilized, the creep curves exhibited primary regimes followed by steady-state creep. In the stress-change experiments in which the stress was increased after establishment of the steady-state creep regime, further primary creep was exhibited. These observations indicated that, in the intermetallics used in this investigation, the creep deformation proceeds by the continued formation of a more creep-resistant sub-structure during the primary stage and by stabilization of this structure by some recovery process or processes during the steady-state stage. For the same stress values, the measured steady-state creep rates were found to be about the same in both the single-stress and the stress-change experiments. This indicated that the steady-state creep was not sensitive to the differences in the prior deformation structure.

3.3. Temperature dependence of steady-state creep rate

3.3.1. Ti_3Al

Steady-state creep rates, $\dot{\epsilon}_s$, were obtained by calculating the slopes of the secondary regimes of the types of creep curves shown in Fig. 2. For Ti_3Al, $\dot{\epsilon}_s$ is plotted in Fig. 3 as a function of the reciprocal of the absolute temperature, $1/T$, for four stress values, 138, 172.4, 207, and 241 MN m^{-2}. The data were represented by parallel straight lines indicating that the rate-controlling thermal-activation process is independent of stress level. From the least-squares slopes of these lines, an average value of 2.23×10^5 J mol^{-1} was obtained for the apparent activation energy of creep, Q_a.

3.3.2. Ti_3Al + 10 wt % Nb

Fig. 4 is an Arrhenius plot showing the temperature dependence of $\dot{\epsilon}_s$ for Ti_3Al + 10 wt % Nb for two stress values, 312 and 138 MN m^{-2}. The data corresponding to the 312 MN m^{-2} stress could be represented by two straight lines having different slopes. Above about 650° C, the straight line had a larger slope and, from a least-square calculation, an apparent activation energy, Q_a, of approximately 3.1×10^5 J mol^{-1} was obtained. Below about 650° C, the straight lines had a smaller slope yielding a value of Q_a equal to

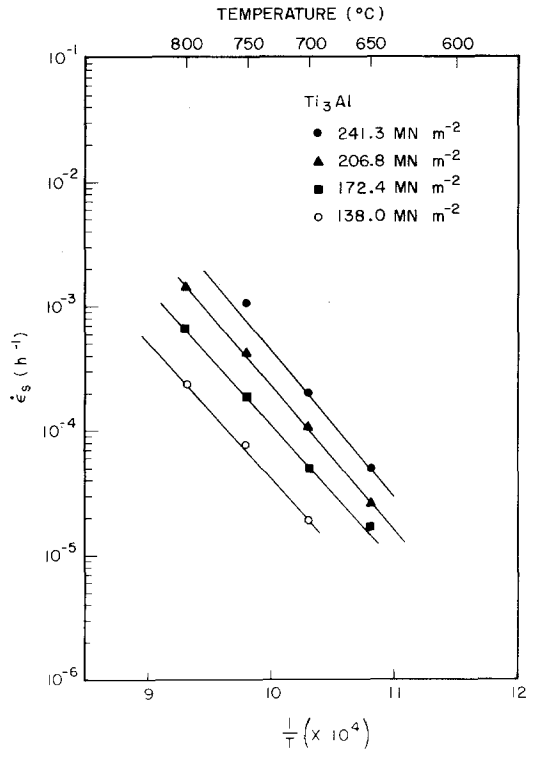

Figure 3 Temperature dependence of steady-state creep rate for Ti_3Al.

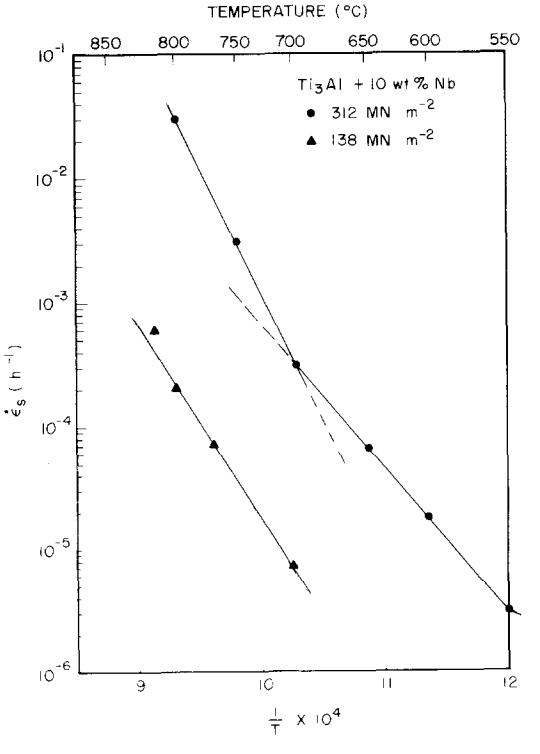

Figure 4 Temperature dependence of steady-state creep rate for Ti_3Al + 10 wt % Nb.

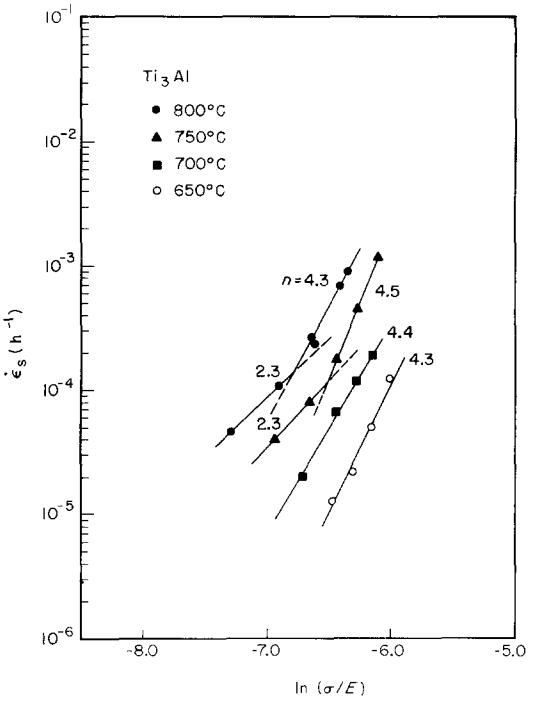

Figure 5 Normalized stress dependence of steady-state creep rate for Ti_3Al.

approximately 1.9×10^5 J mol^{-1}. For a stress value of 138 MN m^{-2}, the creep runs were made only in the 700 to 825° C range, the creep strains being extremely small below 700° C because of the low stress utilized. The data could be represented by a straight line which was very nearly parallel to the straight line for 312 MN m^{-2} creep runs above about 650° C. Thus, above about 650° C, Q_a appears to be independent of stress. Below 650° C, a lower-activation-energy creep mechanism appears to be rate controlling.

3.4. Stress dependence of steady-state creep rates

3.4.1. Ti_3Al

In Fig. 5, values of $\dot{\epsilon}_s$ for Ti_3Al are plotted as a function of ln (σ/E) for temperatures varying from 650 to 800° C. The temperature dependence of Young's modulus, E, has been reported for both Ti_3Al and Ti_3Al + 10 wt % Nb over the temperature range between 25 and 940° C [8]. The fact that the creep data could be represented by straight lines indicates a power-law stress dependence of $\dot{\epsilon}_s$. The data corresponding to 750 and 800° C could not be represented by single straight lines. At stresses below 138 MN m^{-2}, the data fit straight lines having smaller slopes than

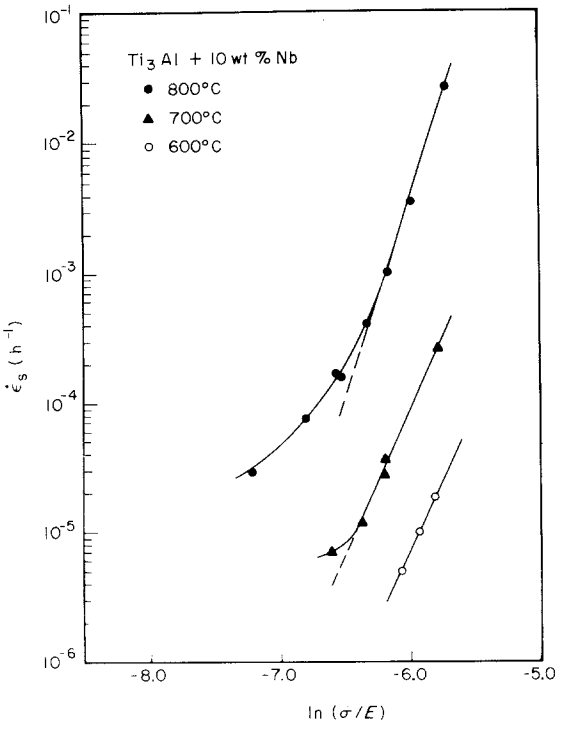

Figure 6 Normalized stress dependence of steady-state creep rate for Ti_3Al + 10 wt % Nb.

those for the higher stresses. This is taken as an indication of a change in the creep mechanism at these low stresses.

3.4.2. Ti_3Al + 10 wt % Nb

In Fig. 6, values of $\dot{\epsilon}_s$ for Ti_3Al + 10 wt % Nb are plotted as a function of ln (σ/E) obtained at 600, 700, and 800° C. From Fig. 6 it can be seen that above a stress level of about 172.5 MN m^{-2}, the data for all temperatures could be represented by nearly parallel straight lines, indicating the power-law stress dependence of $\dot{\epsilon}_s$. Below a stress level of 172.5 MN m^{-2}, the straight lines had a smaller slope for both 800 and 700° C, indicating a change in mechanism. This behaviour is similar to that observed in Ti_3Al except for the fact that in Ti_3Al, the change occurs at a stress level of about 138 MN m^{-2}.

The change in mechanism indicated by the data in Figs. 5 and 6 can be better represented by plotting $\dot{\epsilon}_s$ against (σ/E) on a temperature-compensated basis. A correction in the value of Q_a is required before temperature compensation can be attempted. The physical basis for this correction lies in the fact that, in the Arrhenius plots of Figs 3 and 4, the temperature dependence of E is not taken into account, even though $\dot{\epsilon}_s$ is correlated with $\sigma/E(T)$ in Figs 5 and 6. Lund and Nix [9] have shown that in such a case, the activation energy for creep, Q_c, is given by

$$Q_c = Q_a + \left(nR\frac{T^2}{E}\right)\left(\frac{dE}{dT}\right), \qquad (1)$$

where Q_a is defined as the apparent activation energy obtained from an Arrhenius plot, n is the normalized stress exponent, R is the gas constant, T is the absolute temperature, and dE/dT is the temperature dependence of Young's modulus. The value of dE/dT for most materials is negative and so $Q_c < Q_a$. The values of dE/dT were obtained from the E against T data given in [8] for both Ti_3Al and Ti_3Al + 10 wt % Nb. Taking average stress exponent values of 4.5 and 6 for Ti_3Al and Ti_3Al + 10 wt % Nb, respectively (from Figs. 5 and 6), the average correction values (second term in Equation 1) for the range of creep temperatures were calculated to be about -1.65×10^{-4} J mol^{-1} for Ti_3Al and about -2.48×10^{4} J mol^{-1} for Ti_3Al + 10 wt % Nb. These values are small and therefore, not significant.

The temperature compensation can now be achieved by plotting ln $\dot{\epsilon}_s + Q_c/RT$ as a function of ln(σ/E) for all $\dot{\epsilon}_s$ data for Ti_3Al from 650 to 800° C and for $\dot{\epsilon}_s$ data corresponding to 700 and 800° C for Ti_3Al + 10 wt % Nb. The 600° C data for Ti_3Al + 10 wt % Nb cannot be included because of the lower activation energy shown in Fig. 3. The temperature-compensated plots of Fig. 7 clearly show the change in creep mechanism at lower stresses.

3.5. Phenomenology of steady-state creep

The temperature and stress dependences of $\dot{\epsilon}_s$ for both Ti_3Al and Ti_3Al + 10 wt% Nb indicate that, for the stress and temperature range investigated, $\dot{\epsilon}_s$ can be described by

$$\dot{\epsilon}_s \propto (\sigma/E)^n \exp(-Q_c/RT) \qquad (2)$$

Creep in Ti_3Al is characterized by an activation energy of 2.06×10^5 J mol^{-1} at all stresses and temperatures. The stress exponent, n, has a value of between 4.3 and 5 at stresses above about 138 MN m^{-2}. At temperatures at and above 750° C and at stresses below about 138 MN m^{-2}, the stress exponent has a value of between 2.3 and 2.5.

For Ti_3Al + 10 wt % Nb above 650° C, creep is characterized by an activation energy of 2.85×10^5 J mol^{-1}. Two distinct rate-controlling creep mech-

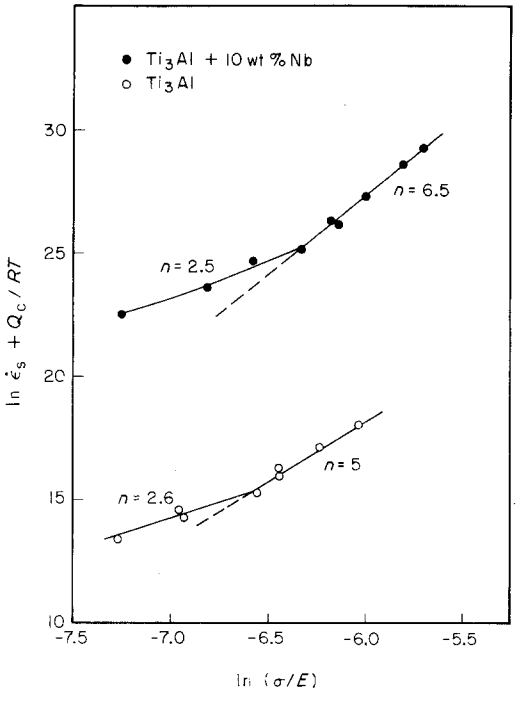

Figure 7 Normalized dependence of temperature-compensated steady-state creep for both Ti_3Al and Ti_3Al + 10 wt % Nb.

anisms are indicated above 650° C, one mechanism having an n value of 6.5 above 172.5 MN m^{-2} stress and the other having an n value of 2.5 below a stress value of 172.5 MN m^{-2}. Below 650° C the creep is controlled by yet another activated process having an activation energy of about 1.9×10^5 J mol^{-1} and a stress exponent of 5.5.

At present, it is difficult to identify which particular creep mechanism is rate-controlling in different temperature and stress regimes; this difficulty stems primarily from the non-availability of diffusion data for Ti_3Al–base intermetallics. The measured creep-activation energies cannot be compared to those for diffusion. At high temperatures and stresses, activation energies of 2.06×10^5 J mol^{-1} and 2.85×10^5 J mol^{-1} for Ti_3Al and Ti_3Al + 10 wt % Nb, respectively, and the stress exponent values of between 4 and 6, indicate that dislocation climb is the most probable rate-controlling process. The change in mechanism indicated at low stresses may be, in fact, a transition regime and, at very low stresses and high temperatures, grain-boundary sliding may be that rate-controlling mechanism.

4. Conclusions

The creep activation energy for Ti_3Al was found to be 2.06×10^5 J mol^{-1} for the stress and temperature range investigated. Addition of Nb increased the activation energy to a value of 2.85×10^5 J mol^{-1} for creep above 650° C and decreased it to a value of 1.9×10^5 J mol^{-1} for creep below 650° C.

The stress exponent for both intermetallics was found to be stress dependent at high temperatures. For Ti_3Al, the stress exponent had a value of between 4.3 and 5 above a stress value of 138 MN m^{-2} and between 2.3 and 2.5 below a stress value of 138 MN m^{-2}. For Ti_3Al + 10 wt % Nb the stress exponent had a value of 6.5 above a stress of 172.5 MN m^{-2} and 2.5 below a stress of 172.5 MN m^{-2}. At low temperatures the stress exponent was found to be independent of stress for both materials, having values of between 4.3 and 5 and of 6.5 for Ti_3Al and Ti_3Al + 10 wt % Nb, respectively.

Due to non-availability of diffusion data at present, it was not possible to identify the rate-controlling creep mechanisms in these intermetallics.

Acknowledgements

The authors wish to thank M. Whitaker, S. Ehlers, and H. Bailey for the preparation of the manuscript. This work was supported in part under Contract F33615-78-C-5037.

References

1. H. A. LIPSITT, R. E. SCHAFRIK and D. SCHECHTMAN, *Met. Trans.* **11A** (1980) 1369.
2. J. C. WILLIAMS and M. J. BLACKBURN, in "Ordered Alloys" edited by H. Kear, T. Sims, S. Stoloff and J. H. Westbrook (Claitor's Publishing Division, Baton Rouge, Los Angeles, 1970) pp. 425–445.
3. S. M. L. SASTRY and H. A. LIPSITT, *Met. Trans.* **8A** (1977) 1543.
4. *Idem, Acta Met.* **25** (1977) 1279.
5. N. S. CHOUDHURY and J. E. HENRY, Systems Research Laboratories, Inc., Dayton, Ohio, unpublished work.
6. H. A. LIPSITT, D. SECHECHTMAN and R. E. SCHAFRIK, *Met. Trans.* **6A** (1975) 1991.
7. M. J. BLACKBURN and J. C. WILLIAMS, *Trans. TMS-AIME* **239** (1967) 187.
8. R. W. SCHAFRIK, *Met. Trans.* **8A** (1977) 1003.
9. R. W. LUND and W. D. NIX, *ibid.* **6A** (1975) 1329.

Recieved 27 March and accepted 1 May 1980.